LA-UR- 00-786

Globally optimized Fourier finite-difference migration method

Lian-Jie Huang and Michael C. Fehler, Los Alamos Seismic Research Center, Los Alamos National Laboratory*

Summary

To image complex structures with strong lateral velocity variations and steep dips, we use a rational approximation of the square-root operator in the one-way wave equation to develop a globally optimized Fourier finite-difference method. The two coefficients in the rational approximation are obtained by an optimization scheme that maximizes the maximum dip angle of the Fourier finite-difference method for a given model. Our optimized method uses the same coefficients throughout a model in contrast to Ristow-Rühl's locally optimized Fourier finite-difference scheme which uses coefficients varying with lateral velocity contrast. The table of coefficients could be huge for a highly accurate optimized scheme. The computational cost of our optimized method is the same as other Fourier finite-difference methods. Our optimized method is accurate for dips with angles of approximately 15°–20° larger than that of Ristow-Rühl's unoptimized Fourier finite-difference method, while Ristow-Rühl's optimized scheme can handle approximately 16° larger dip angles than their unoptimized scheme.

Introduction

Migration methods that use finite-difference of the one-way wave equation can handle arbitrary large velocity contrasts but are only accurate up to a fixed dip angle even in a homogeneous region (Claerbout, 1985). The phase-shift migration (Gazdag, 1978) is accurate up to 90° but it requires a laterally homogeneous velocity model. A hybrid approach, termed the Fourier finite-difference (FFD) method proposed by Ristow and Rühl (1994), has the advantage of both finite-difference and phase-shift methods. The FFD method uses a Taylor expansion of the square-root operator in the one-way wave equation and the expansion is recombined into a rational approximation. Its implementation uses the split-step Fourier (SSF) propagator (Stoffa et al., 1990; Huang and Fehler, 1998) followed by a finite-difference scheme to accurately image structures with large lateral velocity contrasts. Some other Fourier transform based methods, such as the extended local Born Fourier (Huang et al., 1999b), the extended local Rytov Fourier (Huang et al., 1999a), and the quasi-Born Fourier (Huang and Fehler, 2000) methods, are more accurate than the SSF method, but they are less accurate than the FFD method for large lateral velocity contrasts. Another version of FFD (Xie and Wu, 1998) is based on the approximation of the square-root operator using the first order Padé approximation which is the same as Claerbout's 45° or Muir's R_2 apaproximations (Claerbout, 1985). It is less accurate than Ristow-Rühl's FFD method. We refer the Padé-based method to as the PFFD method hereafter.

To increase the accuracy of the FFD methods, one can in principal add additional terms to the finite-difference operator. However, the computational cost of the finite-difference operator increases proportionally to the number of terms added. To increase the accuracy of the second-order FFD method while using only one term in the finite-defference operator, Ristow and Rühl (1994) proposed a locally optimized Fourier finite-difference (LOFFD) scheme in which they optimized a coefficient that varies with lateral velocity contrast. The LOFFD method requires a large table of coefficients for different lateral velocity contrasts that could be huge for a highly accurate optimized FFD.

We propose an FFD method based on a rational approximation of the square-root operator. The form of our FFD scheme is same as that of the PFFD method. However, the two coefficients in the rational approximation used in our FFD method are determined using an optimization scheme that maximizes the maximum dip angle for a given model, rather than using those of the one-term Padé approximation. We give the optimization algorithm, perform the error analysis of our optimized scheme, and present migration images of an impulse response using different methods. Our optimized FFD method does not require a table of the optimized coefficients because these coefficients are fixed for a given model. Therefore, we call it the globally optimized Fourier finite-difference (GOFFD) method. The computational cost of the GOFFD method is the same as the FFD and PFFD method. The GOFFD method is accurate for dips with angles of approximately 15°–20° larger than the FFD method, while the LOFFD scheme can handle approximately 16° larger dip angles than their unoptimized scheme.

Expansion of Square-Root Operator

The one-way wave equation in the frequency-space domain is

$$\frac{\partial P(x,z;\omega)}{\partial z} = i\,Q(x,z;\omega)\,P(x,z;\omega), \tag{1}$$

where P is the pressure and the operator Q is defined by

$$Q \equiv \sqrt{\frac{\omega^2}{v^2(x,z)} + \frac{\partial^2}{\partial x^2}} = \frac{\omega}{v(x,z)} R, \tag{2}$$

where ω is the circular frequency, v is the velocity, and R is the square-root operator given by

$$R \equiv \sqrt{1 - X^2}, \tag{3}$$

with

$$X^2 = -\frac{v^2}{\omega^2}\frac{\partial^2}{\partial x^2}. \tag{4}$$

We expand the square-root operator R in the form

$$R \approx 1 - \frac{a\,X^2}{1 - b\,X^2}, \tag{5}$$

DISCLAIMER

DISCLAIMER

Portions of this document may be illegible in electronic image products. Images are produced from the best available original document.

```
forall θ1, 0° < θ1 ≤ 90°
  forall θ2, θ1 < θ2 ≤ 90°
    • calculate a and b (eqs.17 and 18)
      forall m, 1 ≤ m ≤ m_max
        forall θ, 0° ≤ θ ≤ 90°
          • calculate ε (eq.13)
          • find maximum θ when ε ≤ 1
            (denoted as Θ_m(m))
        end forall θ
        • find minimum value of Θ_m(m)
          (denoted as Θ_{θ1,θ2}(θ1, θ2))
      end forall m
      • find optimized θ1 and θ2 that give
        the maximum value of Θ_{θ1,θ2}(θ1, θ2),
        denoted as Θ (see Table 1)
  end forall θ2
end forall θ1
• calculate optimized a and b using
  optimized θ1 and θ2.
```

Algorithm 1: Procedure to find optimized a and b.

where two free coefficients a and b are determined using an optimization approach described in the next section. The difference between the operator Q given by equation (2) and that in a background media with a velocity of $v_0(z)$ is

$$D = \frac{\omega}{v}\sqrt{1-X^2} - \frac{\omega}{v_0}\sqrt{1-X_0^2} \tag{6}$$

where X_0^2 is given by

$$X_0^2 = -\frac{v_0^2}{\omega^2}\frac{\partial^2}{\partial x^2} = \frac{X^2}{m^2} \tag{7}$$

where the lateral velocity contrast $m(x,z) = v(x,z)/v_0(z)$ is the reciprocal of the refraction index. Making use of equation (5), combining the two fractions into one, and keeping only the first-order term in the numerator and denominator of the resulting fraction, equation (6) becomes

$$D \approx \left(\frac{\omega}{v} - \frac{\omega}{v_0}\right) - \frac{\omega}{v_0}\frac{a\,(m-1)\,X_0^2}{1-b\,(1+m^2)\,X_0^2}. \tag{8}$$

Therefore, equation (2) can be approximated by

$$Q \approx \sqrt{\frac{\omega^2}{v_0^2} + \frac{\partial^2}{\partial x^2}} + \frac{\omega}{v_0}\left(\frac{1}{m} - 1\right) - \frac{\omega}{v_0}\frac{a\,(m-1)\,X_0^2}{1-b\,(1+m^2)\,X_0^2}. \tag{9}$$

The first two terms of this equation are accomplished using the split-step Fourier method and the third term is carried out using an implicit finite-difference scheme.

Optimization

The two coefficients a and b in equation (9) are obtained by minimizing the error of the approximate Q given by that equation. We consider a given velocity v in the following. From

Table 1: Values of a and b for different range of $m = v/v_0$, $1 \le m \le m_{\max}$. Θ in the table is the minimum value of the maximum dip angles for a given range of m.

$m_{\max}$	θ_1	θ_2	a	b	Θ
1.5	18.86	78.76	0.4907073	0.4299809	68.4
2.0	21.89	78.42	0.4875533	0.4319840	66.9
2.5	26.08	77.94	0.4824503	0.4357718	66.4
3.0	28.78	77.39	0.4788818	0.4374196	65.5
3.5	31.41	76.95	0.4750325	0.4401460	64.8
4.0	33.28	76.50	0.4722433	0.4415782	64.0

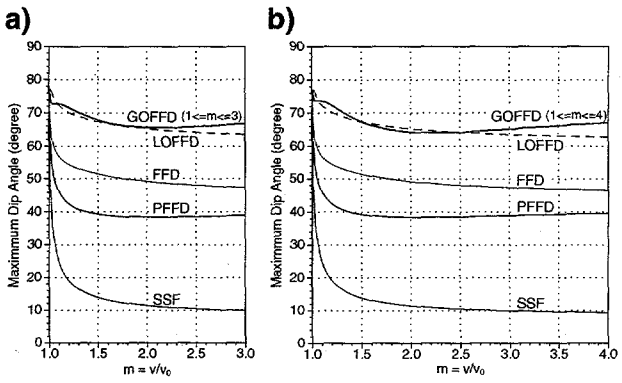

Fig. 1: Comparison of maximum dip angles versus the lateral velocity contrast m for the SSF, PFFD, FFD, LOFFD, and GOFFD method. (a) is for $m_{\max} = 3$ and (b) is for $m_{\max} = 4$.

equations (2)–(4), (7), and (9), and making use of the transformation: $-\partial^2/\partial x^2 \Longleftrightarrow k_x^2$, we obtain the approximate operator Q in the frequency-wavenumber domain given by

$$Q^{\text{app}} = \frac{\omega}{v}\,R^{\text{app}}, \tag{10}$$

with

$$R^{\text{app}} = m\sqrt{1-\frac{\chi^2}{m^2}} + (1-m) - \frac{a\left(1-\frac{1}{m}\right)\chi^2}{1-b\left(1+\frac{1}{m^2}\right)\chi^2}, \tag{11}$$

where the superscript "app" in equations (10) and (11) represents the approximation, and χ^2 is defined by

$$\chi^2 \equiv \frac{v^2}{\omega^2}k_x^2 = \sin^2\theta, \tag{12}$$

where θ is the dip angle. The percentage relative error of Q^{app} is

$$\varepsilon(\chi) = \frac{|Q^{\text{app}} - Q|}{Q} \times 100 = \frac{|R^{\text{app}} - R|}{R} \times 100. \tag{13}$$

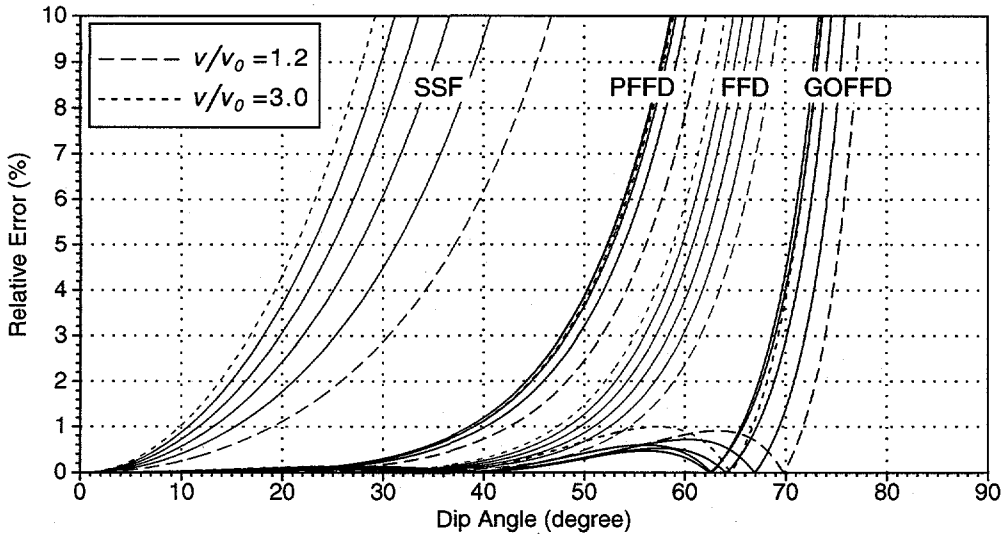

Fig. 2: Comparison of percentage relative errors versus the dip angle θ for the SSF, PFFD, FFD, and GOFFD method when $m = v/v_0$ varies from 1.2 to 3.0 with an interval of 0.36.

From equation (5), we obtain the square-root operator in the frequency-wavenumber domain given by

$$R \approx 1 - \frac{a\chi^2}{1 - b\chi^2}, \tag{14}$$

which is exact when $\chi = 0$, that is, $\theta = 0°$ for propagation along z-axis. We choose equation (14) to be exact at two other angles θ_1 and θ_2. Therefore, we have

$$R_1 - 1 + \frac{a\chi_1^2}{1 - b\chi_1^2} = 0, \tag{15}$$

$$R_2 - 1 + \frac{a\chi_2^2}{1 - b\chi_2^2} = 0, \tag{16}$$

where $R_1 = \sqrt{1-\chi_1^2}$, $R_2 = \sqrt{1-\chi_2^2}$, $\chi_1 = \sin\theta_1$, $\chi_2 = \sin\theta_2$. Solving equations (15) and (16) for a and b yields

$$a = \frac{(1-R_1)(1-R_2)(\chi_2^2 - \chi_1^2)}{\chi_1^2\chi_2^2(R_1 - R_2)}, \tag{17}$$

$$b = \frac{\chi_1^2(1-R_2) - \chi_2^2(1-R_1)}{\chi_1^2\chi_2^2(R_1 - R_2)}. \tag{18}$$

For a given model, the lateral velocity contrast m is bounded within $[1, m_{\max}]$, where $m_{\max}$ is the maximum lateral velocity contrast. The values of a and b are obtained by a search algorithm (Algorithm 1) that maximizes the maximum dip angle at which the error given by equation (13) is 1% when $1 \le m \le m_{\max}$. To search for optimized values more quickly, a larger angle interval for θ_1 and θ_2 is first used to obtain the approximate optimized values for θ_1 and θ_2. Then a smaller angle interval is used to find the optimized value of θ_1 and θ_2 within smaller ranges around their approximate optimized values. Using the optimized values of a and b in equation (9) leads to a globally optimized Fourier finite-difference (GOFFD) scheme.

Using Algorithm 1, we obtain optimized values of a and b for $m_{\max} = 1.5,\ 2.0,\ 2.5,\ 3.0,\ 3.5,\ 4.0$ and tabulate them in Table 1.

Error Analysis

Figure 1 is the comparison of the dependence of maximum dip angle on the velocity contrast m for the SSF, PFFD, FFD, LOFFD, and GOFFD method. For most of geophysical application, the maximum value of lateral velocity contrast $m_{\max}$ is approximately less than 4. For example, $m_{\max} = 2.988$ in the SEG/EAGE 3D salt model, $m_{\max} = 2.544$ in the Marmousi model. Therefore, we select $m_{\max} = 3$ and $m_{\max} = 4$ for the comparison (see Figure 1a and Figure 1b). The SSF method can handle very small dip angles for large lateral velocity contrasts. The maximum dip angle for the GOFFD method is approximately 26° larger than the PFFD method, 15°–20° larger than the FFD method. For large lateral velocity contrasts, the maximum dip angle for the GOFFD method is gradually larger than that of the LOFFD method.

In Figure 2, we compare relative errors versus the dip angle θ for the SSF, PFFD, FFD, and GOFFD method. For a given level of the error, the maximum dip angle progressively increases among methods in the following order: SSF, PFFD, FFD, and GOFFD.

Impulse Response Migration

A homogeneous medium with $v = 4500$m/s is used to migrate an impulse response at the upper center of the model. A reference velocity of $v_0 = 1500$m/s was used during migrations so the lateral velocity contrast in the whole model is 3.0. Figure 3 shows the migration images obtained using the SSF, PFFD, FFD, and GOFFD method. For this large velocity contrast, the GOFFD method can handle the largest dip angle